Investigation into the Viability

of a

Magnetic Thin Film as an Analog, Nonvolatile Memory Device

Matthew Grein
University Undergraduate Fellow, 1992-1993

Texas A&M University
Department of Electrical Engineering

APPROVED

Fellows Advisor 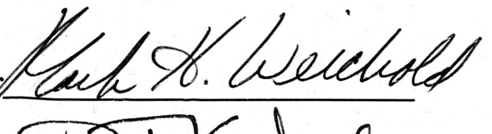

Honors Director 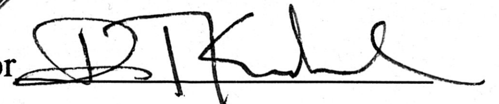

ABSTRACT

Investigations into the Viability of a Magnetic Thin Film as an Analog, Nonvolatile Memory Device

A %50Co-50%Fe magnetic film of 1000Å has been used as the memory element fabricated on a silicon substrate to be used as a nonvolatile memory with read/write capabilities. A Hall element has been employed to detect the memory state of the device .

The devices suffer from extreme leakage currents and breakdowns due to an erroneously prepared mask used during photolithography. This limits any measurements of the memory states to yield information only on the static behavior of the magnetic film . At the time of this writing, conclusive evidence is not available to argue for the viability of the device as an analog memory. However, along the way, some important findings have been reached:

1. The Hall element worked and contributes a negligible voltage drop during measurements of magnetic induction.
2. The Fe-Co alloy used showed a mechanical resilience through standard silicon processing.
3. During the annealing process in H_2/N_2 forming gas, films of 1000Å were observed to have rather smooth, homogeneous surfaces when viewed at 1000 X after 5 hours at 500°C. After 10 hours at the same temperature, the films appeared to be rather rough and heterogeneous. This evidence supports other experimental evidence indicating the difference in material and magnetic properties when comparing thin films to bulk material. Further, the evidence indicates the need for further research on characterizing the annealing of thin films and exploring other properties unique to thin-film materials.

I. Introduction

A. Background

Kantimahanti[1] fabricated and demonstrated a novel, non-volatile memory device capable of reading/writing a digital signal via magnetic, thin film (1000 Å) of 50% Co-50% Fe deposited on a silicon substrate. The thesis proved the viability for nonvolatile memory applications in thin magnetic films on silicon for use as digital memory elements. Too, Kantimahanti demonstrated the integrity of the iron-cobalt alloy during routine silicon fabrication procedures. However, the magnetic film appeared to delaminate upon annealing, and the final device was not completed.

B. Scope

The effort this research is to complete and modify Kantimahanti's digital device to explore its potential as an analog memory storage device. Friedlander and colleagues[2] at Purdue demonstrated that a bulk sample of permalloy *could be used* as an analog device and were able to write to almost one hundred intermediate states of magnetic induction consistently. In this context, an interesting comparison between the minor loop behavior between bulk and thin films can be posed. The motivation for using a thin film is in this research effort lies in the exploitation of the uniaxial anisotropy, giving rise to faster switching speeds than possible in the bulk material. Note, however, that no attempt is made here to measure the switching speed of the film; rather, attempts here are only made to demonstrate the viability of utilizing thin ferromagnetic films as analog devices as similarly demonstrated my Friedlander in bulk ferromagnetic materials. The nature of this work is, in large part, experimental: while much effort has been expended on understanding magnetic phenomenon in thin film materials since the 1950's, many

questions remain unanswered, among them: a complete understanding of the mechanisms for domain reversal, the effects of heat treatments/annealing on the hyteresis curve, and mechanical properties of the films regarding adhesion to substrates and internal stress, to name a few.

No attempt will be made here to devise a mathematical model for the minor loop behavior in thin films as Jiles and Atherson[3] did for bulk materials. Ossart *et al.*[4] compared the behavior of various hysteresis models, including the Mayergoyz model[5] (an extention of the Preisach model) and Hodgdon model[6], with experimental results in a bulk ferromagnetic alloy. Carpenter[7] demonstrated that the Jiles Atherton hysteresis model could be improved to simulate the dynamic behavior of minor loops in ferromagnetic materials. While no such attempt to model the static/dymanic characteristics is made here for a thin ferromagnetic material, the results could be used for verification of such a model. The main thesis is to demonstrate the viability of minor-loop behavior in a thin film of a Fe-Co ferromagnetic alloy. Section II. demonstrates the proposed operation of the analog device; section III. describes the physics of thin ferromagnetic films and gives a general overview of relevant theoretical considerations of magnetic phenomena; section IV. gives a brief technical summary of the Fe-Co alloy used as the memory element; section V. gives a brief overview of the fabrication of the device; section VI. reports on the testing equipment; and sections VII and VIII. provide discussions on the data and conclusions of the total effort.

II. Proposed Device Operation

The following is a simplified overview of how the proposed device should operate. The basic design, operation, and fabrication are taken from a thesis by Kantimahanti[1]. Figure 1 is a top view of the device. Figure 2 is the characteristic hysteresis of the magnetic material used as the memory element as described in detail in section III.

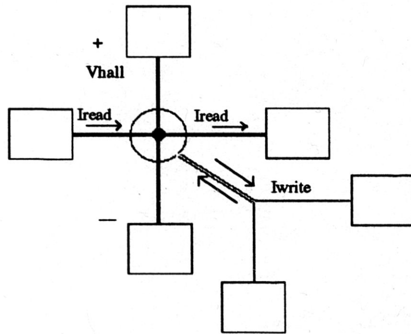

Figure 1 - Top view of memory device

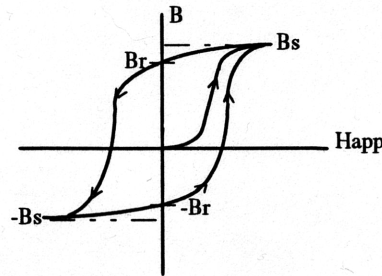

Figure 2 - Magnetization curve exhibiting hysteresis

According to the Hall effect, as a reading current I_{read} is passed through the metallic conduction pads underneath the magnetized sample consisting of a Hall sensing element, a voltage V_{hall} develops across the device according to the Hall effect[8]:

$$V_{hall} = \frac{B}{qnd} I_{read} \qquad \text{(II-1)}$$

where I_{read}=reading current density, A/m^2
B=magnetic flux density, Wb/m^2
q=electronic charge, C
n=carrier density , cm^{-3}

By keeping I_{read} constant, information on the memory state of the device is contained in V_{hall} . If one could change B selectively, then one would have a device that could store

analog values within the range of $\pm B_r$, where B_r is the remnant magnetic flux density (or induction) as seen in figure 2. To write to the device, a current loop shown in figure 1 was built to surround the magnetic dot. By pulsing the loop with a current of a set amount given by

$$H_{app} = \frac{1}{2r} I_{write} \quad \text{(II-2)}$$

where I_{write} =writing current
H_{write}=induced magnetic field
r =radius of the writing loop

The generated magnetic field in the loop exerts a magnetic force on the memory element, thus changing B [9]. As shown in figure 2, ferromagnetic materials will retain a non-zero magnetized state even when I_{write} is zero.

B. Demonstration of Analog Behavior

To illustrate the device's operation, assume the magnetic material is initially in the $-B_r$ state. Upon application of an applied field of magnitude h_1 (via a current pulse of magnitude I_1), the flux density magnetism increases to b_1 along the major loop as shown in figure 3. If the applied field h_1 is less than that needed to saturate the material and is then reduced to zero, the residual magnetism cannot settle back into its former state of -B_r; rather, the residual flux follows a *minor loop* as shown and settles into b'. From (II-1), it is seen that upon application of a standard reading current, the voltage for this remnant magnetic flux density can be utilized as just one of many analog states between $\pm B_r$.

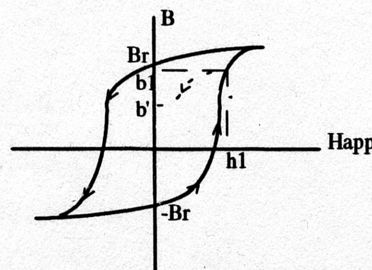

Figure 3 - Demonstration of a hysteretic minor loop in a ferromagnetic material

III. Physics of Thin Films

A. General Macroscopic Behavior of Magnetic Materials (taken from Solymar *et al.*[8])

In a vacuum, the macroscopic relationship between the magnetic flux density (Wb/m^2) and magnetic field is given by

$$B = \mu_o H \quad \text{(III-1)}$$

where μ_0 = permeability of free space

In the presence of a given material, the expression is modified to account for the internal field within the material:

$$B = \mu H \quad \text{(III-2)}$$

where M = magnetic dipole moment per unit volume, or magnetization
μ_r = relative permeability

The constitutive relationship between magnetization and the magnetic field is given by

$$M = \chi H \quad \text{(III-3)}$$

where χ = magnetic susceptibility

so, after substituting into (III-2),

$$B = \mu_o \mu H$$

or,

$$B / B_o = \mu \quad \text{(III-4)}$$

where μ_r= relative permeability

Notice that μ_r and χ are material properties. Relative permeability is an indicator of a material's tendency to either oppose or align with an applied field. For diamagnetic

materials, μ_r is slightly less than one; in paramagnetic materials, μ_r is slightly greater than one.

While both paramagnetic and diamagnetic effects are exhibited in all materials to some degree, some materials exhibit properties of ferromagnetism and its converse, antiferromagnetism, that dominate magnetic behavior. Relative permeabilities for these materials can be on the order of thousands or millions--these are the permanent magnets; examples include iron and nickel. The magnetic moments in these materials are spontaneous; that is, strong magnetic dipoles exist even in the absence of an applied field. This suggests the existence of some regular arrangement of magnetic dipoles in the material itself.

For ferromagnetic materials, the relationship must be modified to include the effects of an internal field--only a quantum mechanical approach can account for the most basic of observed magnetic phenomenon[11]. It turns out that[8]

$$M = N_m u_m L\left\{\frac{u_m u_0}{kT}(H + \lambda M)\right\} \tag{II-5}$$

where M = magnetization
N_m = magnetic dipole density
u_m = magnetic moment
λ = Weiss constant
L{ } = Langevian function

One can solve (II-5) for the magnetization for any given value of H (the plot of L{ } is well known). Note that at $H = 0$ (absence of an applied field), there exists a non-zero magnetization--the material will exhibit a magnetic flux density even when the applied field has been turned off.

B. Microscopic Behavior

The magnetic moment, M, has three principal sources: electron spin, electron orbital angular momentum about the nucleus, and the change in the orbital moment induced by an externally applied magnetic field. According to the Lamor theorem, the orbiting electrons generate a magnetic moment proportional to their angular momentum:

$$\mu_m = \frac{q}{2m} L$$

where μ_m = magnetic moment
L = angular momentum of a single electron

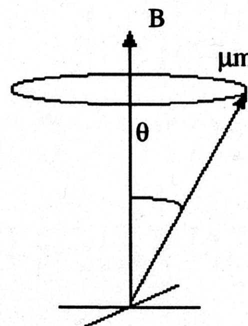

Figure 4 - A magnetic dipole precessing in a magnetic field

Consider an applied magnetic field at an angle of theta to a magnetic dipole as shown in figure 4. The dipole will experience a torque of $\mu_m \times B$, and since the angular momentum is proportional to the dipole (but opposite in sign), the dipole will precess about an axis of rotation oriented at θ with respect to the applied magnetic field[8]. In the absence of losses, the angle ofprecession will remain constant; however, in the presence of losses some energy associated with the angular momentum will be gradually lost. Hence, the dipoles will eventually line up with the applied magnetic field, although not completely due to the energy contributions of thermal vibrations[8]. Note that if a field is applied directly opposite to the magnetic dipoles, the torque $M \times H$ is identically zero[10].

C. Domain Structures

1. Domain Walls, Static Behavior

There exist localized regions called domains within our ferromagnets where the magnetic moments are completely aligned with each other. Landau and Lifshitz showed that the domain structure follows from the contributions of various energies--exchange energy (energy of magnetic dipole coalignment), anisotropic energy , and energy of magnetic dipole formation[11]. Each of the domains are separated from one another by high energy barriers resulting from the transition from one region at a particular magnetization to the next. The directions of magnetizations are believed to switch gradually across these walls as conceptualized in figure 5. While the exact configuration of the domains in neither

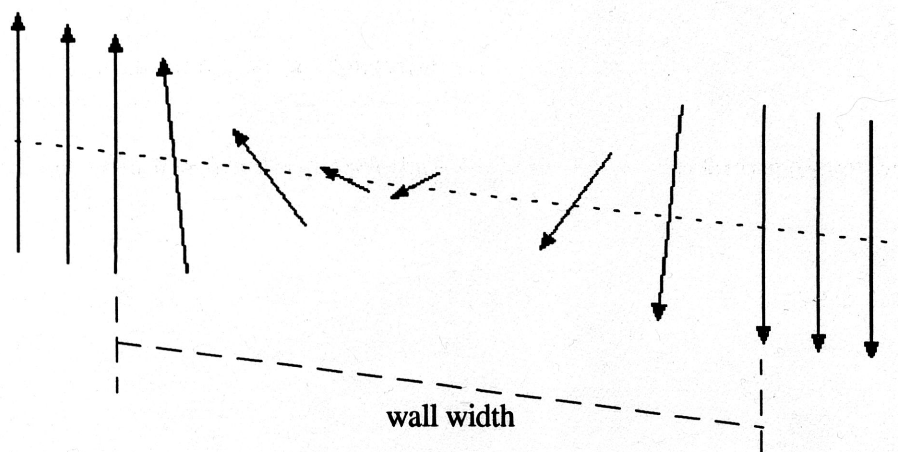

Figure 5 - Rotation of magnetic moments across a domain wall[8]

predictable nor uniform in the ferromagnetic materials, the net effect of the domains is always to create a more favorable, lower energy state. It turns out that these domains are stable only below a certain temperature--the Curie temperature, Tc--and if surpassed, the material behaves as a paramagnetic material and loses its ferromagnetic characteristics.

The type of domain walls differ significantly in thin films as compared to bulk materials due to the shape anisotropy incurred by the extreme thinness of the film compared to other dimensions[12]. As shown in figure 6, the Block walls are oriented such that the magnetization is normal to the plane of the film[11]. Thus, in order to change from one state to the next across the wall, the moments must rotate *in the plane of the film* as opposed to a perpendicular rotation in bulk materials.

2. Domain Wall Motion, Dynamic Behavior, and Hysteresis

Recalling that an applied magnetic field is amplified in the presence of a paramagnetic or ferromagnetic material ($\mu_r > 1$), the increase in the net magnetic moment takes place by two independent processes: in weak applied fields, the volume of domains favorably oriented with the applied field expand at the expense on unfavorably oriented domains. In strong fields, the domain magnetization rotates in alignment with the applied field--see figure 7. The boundaries of the domains are pinned in their positions by impurities. As a field is applied with greater and greater strength, enough

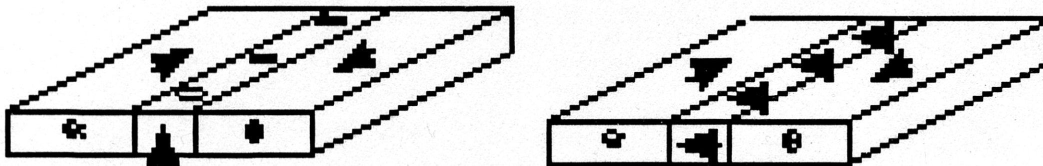

Figure 6 (a) Block wall and (b) Néel wall in a thin film. Magnetization in Block wall is normal to plane of the film; in the Néel wall, the magnetization is parallel to the surface.

energy will be present to free the domain wall from its anchor. The walls themselves move in discontinuous movements--Barkhausen jumps--and will pin themselves to any other impurities in the sample. Notice that the process is irreversiblethat is, reduction of the applied field to its previous value will not yield the same internal field. This is the basis for the hysteresis phenomenon observed in magnetic materials.

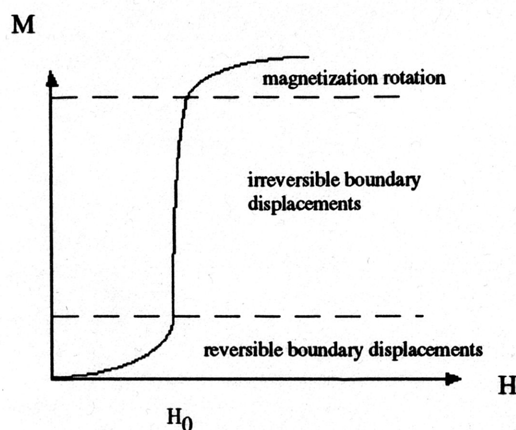

Figure 7 - Magnetization curve[11]

Hysteresis curves like that sketched in the previous figure are mapped according to applied fields that drive the materials into saturation. One can ask what state the material will be in if only driven to only a fraction of H_c. As seen in figure 7, once H_0--the threshold for irreversibility--is surpassed, the state of the material can not return to its previous state; rather, it follows a path as exhibited in figure 3. These pathways are highly repeatable and will be retraced given a similar driving applied field.

D. Crystallographic Orientation and Magnetocrystalline Anisotropy

1. Crystallographic Orientation

Recalling the nature of the electronic origins of magnetic behavior, magnetic phenomena are strongly dependent on crystal structure. Thus, magnetic properties can be described as anisotropic in all polycrystalline materials--an applied field will have a greater effect on the magnetization in certain directions as opposed to others. The difference in energies required to magnetize a material between directions is referred to as the anisotropy energy. The origin of this anisotropy is quantum-mechanical, stemming from

the interaction of the spin and orbital angular momenta of electrons by nonhomogeneous crystalline fields and overlapping wave functions associated with the neighboring atoms of the crystal lattice. The crystal structure dictates the magnitude of anisotropy in all magnetic media. The Fe-Co alloy exhibits a cubic anisotropy in the bulk material, varying along the <100>, <110>, and <111> planes[12].

2. Anisotropy in thin films

In thin, single-crystal, ferromagnetic films, it has been experimentally proven that there exist "easy" and "hard" directions with respect to the crystalline axes where the anisotropy energy, E_k, is minimized and maximized, respectively[13]. Here, we are most concerned about the sources of *perpendicular anisotropy*--that is, either the easy or hard axis is directed perpendicularly to the surface of the film. Positive anisotropy (or positive K) refers to the *easy* axis oriented perpendicularly to the surface. Given that the magnetization of these thin-films is dependent on the anisotropy magnetization direction, considerable effort will be devoted here to an discussion of the possible sources of anisotropy.

a. Origins of Anisotropy

Griffith and Standley[14] along with MacDonald[15] demonstrated that perpendicular anisotropy is dependent on the isotropic planar tension which is a function of film thickness. Based on studies of pure iron and 55%Ni-45% Fe thin films (Permalloy), SooHoo[12] postulated that one possible source of anisotropy is due to magnetostriction. Knorr and Hoffman[16] demonstrated that in iron films, an easy axis formed perpendicularly to the inclined deposition beam. Based on these and similar findings, it is reasonable to conclude that our sputtered thin films of Vacoflux should exhibit some positive K.

There exists a number of independent factors contributing to the anisotropy in thin films, including temperature during deposition, formation/annealing/cooling in a magnetic field, substrate material, substrate temperature, oxygen concentration in deposition chamber, and others that can directly affect the magnetic properties of the thin film[12].

b. Effects of anisotropy on hysteresis

We can express the free energy of these thin-film ferromagnets with respect to figure 8 :

$$E = K\sin^2(\phi-\alpha) - H_{\parallel}M\sin\theta\cos\phi - H_{\perp}M\sin\theta\sin\phi + 4\pi M^2\cos^2\theta \qquad \text{(III-5)}$$

where E =free energy
K=anisotropy constant
$(\phi-\alpha)$ =angle M makes with the easy direction
$H_{\parallel}$=longitudinal applied magnetic field
$H_{\perp}$=transverse applied magnetic field

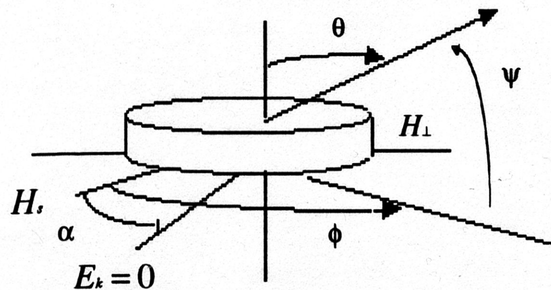

Figure 8 - Anisotropic thin film related to spherical coordinates[10]

Consider the case for α=0; that is, the easy axis aligned with the longitudinal field, $H_{\parallel}$. Let θ=0 and $H_{\parallel}$=0; that is, the longitudinal field is aligned with the easy axis (where E_k=0). The plot in Figure 9 is a plot of the magnetization curve $M\sin\phi$ vs. $h_{\perp}$, where the

transverse field has been normalized to $H_{\perp}M/2K$, where $2K/M$ is defined as the anisotropy field. Notice that the magnetization direction changes with $H_{\perp}$--the hysteresis loop is completely reversible. When the applied field is relaxed, M switches back to its original position. Now consider the hysteresis in the longitudinal direction: let θ=0, $H_{\perp}$=0, and plot $M\cos\phi$ vs. h. Notice that now, the magnetization M is irreversible--it does not move to its original direction once the applied field is relaxed

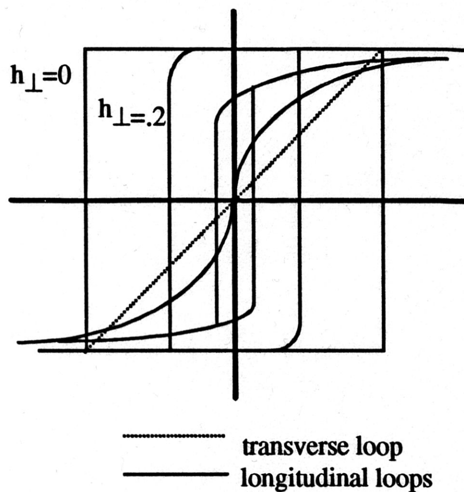

Figure 9 - Theoretical hysteresis with variation in direction of H

Now, as a third case, consider the effects of increasing $h_{\perp}$ from 0 to $h_{\perp} = HM/2K$. The plot in figure 9 shows that as the transverse field is increased, the hysteresis gradually changes from an irreversible square loop to a completely reversible S-shaped curve. The importance of this result lies in this: a field applied perpendicular to the easy axis is will change the coercive force parallel to the easy axis[10]. Considering the toroidal geometry of our writing loop, if the easy axis of the sputtered Vacoflux lies completely in the plane of the film, then no hysteresis will be observed--the memory device will instantaneously forget any information written to it. But, noting the existence of positive K (easy axis out of the plane) observed in thin films of iron, nickel, and their alloys as noted above, it is expected that the Fe-Co Vacoflux will exhibit a positive K as well, thus ensuring a nonreversible hysteresis--a memory that doesn't forget.

3. Magnetic Annealing

To engender the bistable character of a uniaxial internal anisotropy and create an easy and hard direction of magnetization, annealing process have been carried out, typically at high temperatures below the Curie point in the presence of a magnetic field[12]. Graham demonstrated that the binary and ternary alloys inclusive of iron and cobalt showed the largest magnetic annealing effects[17]. As it turns out, the effective field in producing the new anisotropy is the local field of the magnetic material itself that exists as all temperatures below the Curie point. Thus, it is possible for some materials to develop a bistable anisotropy in the absence of and applied magnetic field.

The annealing times and temperatures differ greatly between the bulk material and the thin film[12]. Segmüller[18] demonstrated that Permalloy annealed at temperatures as low as 350°C showed a change in anisotropy. As an additional note, Banks *et al.*[19] observed that the saturation magnetizations in a magnesium ferrite film could be engineered through a range of values between 2100 gauss and 350 gauss by quenching and slow-cooling, respectively.

E. Demagnetization

A thin film has an infinity of states with almost zero demagnetizing energy with no barriers between them, indicating that the time required to switch the magnetic orientation of the dipoles is small[10]. As reported by many researchers near the close of the 1950's, three different mechanisms explaining the reversal process were observed and identified[10,20,21]: domain wall motion, incoherent rotation, and coherent rotation. The reversal process is a strong function of the applied field--if the switching field is much greater than the coercive force, the last (and fastest reversal) mechanism is observed.

Coherent rotation is a phenomenon unique to thin films and has not yet been observed in thick films.

Notice that from a discussion on the operation of the memory device, fields smaller than that required to saturate the material must be employed to settle into the intermediate states between $\pm B_r$. It has been shown that at these low fields, the switching mechanisms are dominated by domain wall motion that starts from nuclei of reversed magnetization at the edges of the film[12]. At these edges, there exists a gradient imposed by the inescapable presence of impurities during the processing of the material.

IV. Material selections

The optimal characteristics for our analog device are 1) a large flux density enabling a large number of states between $\pm B_r$, and 2) a small B/H gradient to allow for practical programming of the minor loop by means of a pulse current on the order of the coercive force. On the first criteria, cobalt-iron alloys exhibit the highest saturation flux density of most commercial materials, thus leaving a large number of states between the maximum and minimum flux densities[22]. On the second, the Vacoflux Z (50%Co-50%Fe supplied by Vacuumschmelze, GMBH) in bulk material exhibits a rather square hysteresis, a property enhancing its desirability for digital (two-state) switching applications, but rendering it almost impossible for use as an analog device. However, when the Vacoflux Z is sputtered or vacuum deposited, the hysteresis rounds off to that shown qualitatively in figures 2 and 3 corresponding to the commercial properties of Vacoflux 48, enabling the possibility for programming the device with analog values[23].

Material Specifications for Vacoflux 48 :

Permeability @4mA/cm	Static Coercivity	Saturation Flux Density	Saturation Magnetostriction
1200	.4 A/cm	2.35 T	$+70 \times 10^{-6}$

For the geometry of our device, the static coercivity corresponds to an I_{write} on the order of 2.16 mA (from equation II-2).

V. Fabrication

The fabrication of the device was carried out in Solid State Laboratories of the Solid State Electronics Division located in the Zachry Engineering Center, Texas A&M University.

A. Device dimensions

Six 2 cm X 2 cm samples were fabricated containing 64 memory elements per sample. Referring to figures 1 and 10 , the dimensions are as follows:

Memory device:	1000 Å thick, 15 µm diameter
Programming loop:	6500 Å thick, 3 µm wide
bulk oxide:	6300 Å thick
thin oxide:	2900 Å thick
diffusion region:	1.8 µm junction depth
bond pads:	123 μm^2

B. Fabrication Process

A detailed fabrication scheme of the memory device has been thoroughly discussed elsewhere[1]; thus, only brief mention of it shall be included here. Figure 10 is an overview of the fabrication process.

Some problems were encountered during processing . Upon removing four of the samples from the Posistrip 830, it was observed that the magnetic film did not remain on the samples. The two other samples run through the exact same process but in a different

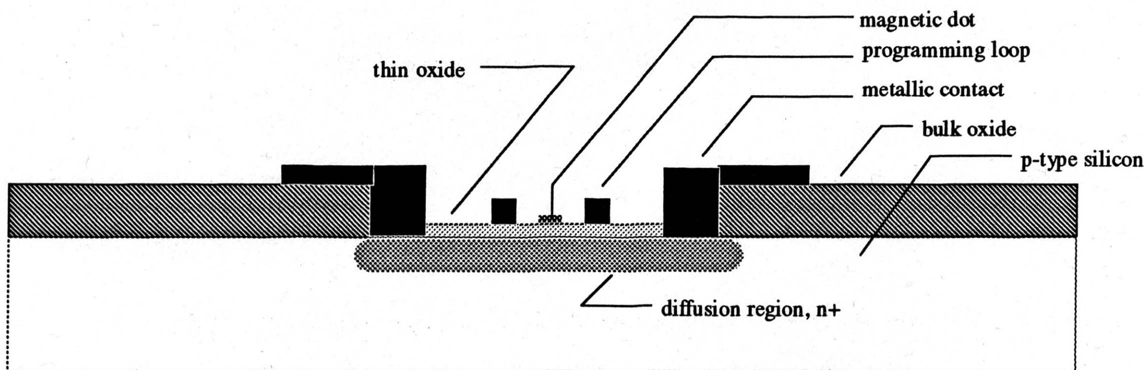

Figure 10 - Cross section of the memory device (not to scale)

batch remained intact. One plausible explaination could be that the Posistrip attacks the Vacoflux. To test this, a sample of the magnetic material was immersed in Posistrip for twenty minutes at 100°C--the Posistrip did not appear to attack the Vacoflux. Another possibility: the O_2 descumer dry-etched the material. However, the protective photoresist on top of the magnetic dot would have to have been etched first. Noting that the thickness of the AZ5214E photoresist protecting the Vacoflux was on the order of 1.2 μm and the etching rate of AZ5214E in the O_2 descumer is only 2500Å/min, the two minute exposure in the descumer would not have been sufficient. However, the assumption that the photoresist was distributed across the wafer evenly may not be valid. Considering that the use of an adhesion promoter is required to marry the organic components of the photoresist with the inorganic substrate, perhaps very little photoresist remained on the magnetic dots during spinning--this would support the argument for the dry-etching in the O_2 descumer. Also, given that the two surviving samples were prepared in different solutions of Posistrip 830, it could be argued that some renegade chemicals happened to be present in the beaker to attack the Vacoflux. Based on studies on the behavior of magnetic thin-films on quartz glass carried out as early as the 1950's, it is not expected that the adherence of the magnetic film to the substrate (at non-extreme temperatures or stresses) should be problematic.

1. Dice six 2cm ⑨ 2 cm [111] p-type wafers, 402 Ω/sq, via mechanical dicing saw.
2. Degrease the wafers in acetone, trichloroethene, pirahana mixture (70 parts 30% sulfurinc acid, 30 parts 30% H_2O_2), isopropanol, heated DI water, methanol
3. 1st Oxidation: 5/75/5 dry/wet/dry @1050°C.
4. Photolithography, image reversal. Define diffusion regions (see appendix).
5. Etch oxide in buffered oxide etch (BOE) for 7 min.
6. Strip photoresist in Posistrip 830 @95°C for 8 min.
7. $POCl_3$ diffusion, 15 min. @950°C.
8. 2nd Oxidation and Drive-in 10/15/10 min. dry/wet/dry @1050°C.
9. DC Sputter Vacoflux @conditions, 1000Å (see appendix).
10. 2nd Photolithograpy, positive. Define magnetic dot.
11. Vacuum hardbake photoresist for 1 hr. @135°C.
12. Etch pattern in etchant (see Appendix).
13. Strip photoresist in Posistrip 830 @95°C for 8 min.
14. 3rd Photolithography, image reversal. Define contact windows.
15. Oxide etch in buffered oxide etch (BOE) for 4 min. Open contact windows to substrate (see appendix).
16. Oxygen descum for 2 min. @135°C, 100Watts, 50sccm O_2.
17. Strip photoresist in Posistrip 830 at 95°C for 8 min.
18. Anneal @500°C for 10 hours in H_2/N_2 forming gas.
19. 4th Photolithography, image reversal. Make metallic contact and form current loop.
20. e-beam aluminum evaporation of 6500Å (see appendix).
21. Aluminum liftoff. Agitate in aetone.
22. Sinter/Anneal in H_2/N_2 forming gas @475°C for 15 min.

Figure 11 - Process flowchart for memory device

C. Heat Treatment

Following from the discussion on the effects of heat treatment in section II., an experimental procedure was followed in annealing the device. While the proper heat treatment of the bulk material is well understood and documented, the case is not so for thin films. It has been shown and previously noted that the annealing times and temperatures are much lower than that for bulk materials. Kantimahanti's annealing

process carried out under conditions appropriate to the bulk material (820°C in N_2, 4-5 hours) resulted in the delamination of the thin magnetic films.

Six test pieces were blanket coated with 1000 Å of Vacoflux to empirically test appropriate conditions for annealing. Three samples were annealed under 10^{-6} Torr vacuum at 500° C for 5 hours, and three others were annealed in a H_2/N_2 forming gas at atmospheric pressure at 500° C for 5 hours. Three separate air-cooling stations were prepared to cool the samples at varying rates; one sample annealed under vacuum and one annealed in the forming gas were placed at each station. Each was observed under microscope at high magnification to identify any noticable changes; specifically, to look for changes in the grain boundaries. At a resolution of 1000X, no noticeable differences between samples were observed; however, it could be seen that the magnetic dots did appear to be homogeneous and no evidence of peeling or delamination was observed. The scanning electron microscope could not resolve any recognizable features due to the charging up of the large amount of oxide in proportion to the small amount of magnetic material.

To experimentally test the effects of different annealing processes on the static/dynamic behavior of the memory elements, one of the remaining samples was annealed @500°C for 10 hours in H_2/N_2 forming gas, while the other sample was not annealed. Note, however, that it was later annealed during the sintering of Al @475°C for 15 min.. The magnetic material annealed @500°C for 10 hours, unlike the test samples annealed for only 5 hours, appeared to be heterogeneous and exhibited a very rough surface as determined via inspection at 1000X. Noting the significant role that grain boundaries have on the magnetic properties of materials, it is expected that, based solely on an optical comparison of the two samples after annealing, their behavior will be noticeably distinct.

VI. Test Set-up

A. Equipment Set-up

The completed memory devices were tested via the following configuration:

I_{read} -	HP 6209 B DC Power Supply
	Westinghouse DC galvanometer
I_{write} -	HP 6209 A DC Power Supply
	Fluke 77 Digital Multimeter
V_{hall} -	Fluke 8010A Digital Multimeter

The device was mounted on a Wentworth 4-point probe station modified to 6 points. A Type 576 Tektronic Curve Tracer was employed to obtain I-V data.

B. Constraints on the testing structures

The mask set used during the photolithography stages was flaw to the extent that the metal contact of one of the current writing paths was exposed *directly on top of the silicon,* creating a diode where isolation was needed. As a result, the fields created at this junction will obscured any other readings made through the Hall element and introduced spurious field to the environment about the magnetic memory. Any attempt at recording real time data--that is, establishing a DC writing current and concurrently reading the Hall voltage to obtain information about the state of the device--was inherently flawed. Plots of the I-V characteristics showed that these contacts acted as perfect diodes. To test for device isolation, the I-V characteristics were plotted between two separate metal contact pads on two adjacent devices. The devices appeared to be isolated enough to support static measurements on the memory devices.

Measurements were made in the following manner: I_{write} was cycled between large currents to generate fields on the order of 50 A/cm (~100 times the coercive force) to initially saturate the material. After three to four cycles, V_{hall} was measured using a .1

mA I_{read} to find $-B_r$, the saturated flux density. To ensure that switching between the maximum and minimum flux densities ($\pm B_r$) was occurring, a large pulse in the positive direction on the order of 55 A/cm (300 mA) was applied, then the V_{hall} was measured. Following, a pulse of -55 A/cm was applied to drive the device into negative saturation, and again the Hall voltage was measured in this relaxed state.

VII. Discussion of the Results

Figure 12 demonstrates that the Hall element works as designed. Using the I-V curve tracer, it was observed that there exists an effective 1 kΩ between two metallic contact pads thorough the Hall element. At a reading current of .1 mA, this corresponds to a voltage drop of 100 mV across the Hall element.

Given that the remnant saturation density of Vacoflux is 2.5 T, then the corresponding Hall voltage in as determined by equation II-1 is 1.9176 Volts; thus, the voltage drop incurred by the use of the Hall element accounts for $.1/1.9 \times 100 = 5\%$, an acceptable error in our measurements of saturation flux density.

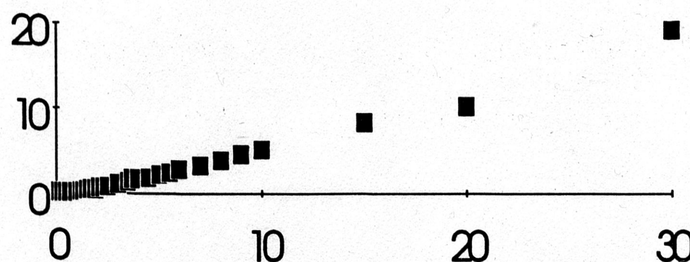

Figure 12 - I-V of the Hall device

At the time of this writing, the memory elements were just entering the testing stage. At present, it has been observed in preliminary testing that the magnetic dots are being magnetized and have been shown to maintain their states even after being in saturation fields 100 times that needed to cause a reversal in the magnetization of the films. As of this date, not enough data has been collected on the difference in static/dynamic behavior between the two samples--one annealed for 10 hours @500°C, the other annealed only for 15 min. @450°C

VIII. Conclusions

It was determined that the annealing process for the Fe-Co alloy should not extend to 10 hours @500°C, and that an anneal carried out for only 5 hours appeared to not stress the material and resulted in a smooth material. It is noted how this contrasts with the annealing process for the bulk material: 4-5 hours @820°C. This may be used as evidence for the actual lowering of the Curie temperature between the thick and thin films. Also, has been shown that the structural integrity of the thin magnetic film was resilient enough to withstand some of the most basic processes encountered in semiconductor manufacturing, such as good adherence to a thermally grown SiO_2 layer and an ability to be patterned and stripped of photoresist without peeling. Further testing, including a redesign of the mask sets used to pattern during the photolithography stages, will be required to make any definitive conclusions on the viability of the device as an analog memory device.

Acknowledgements

The author is indebted to his advisor, Dr. Mark Weichold, for his patience, his time, and his trust and faith in me and my abilities. I also thank Arjun Kantimahanti for his devotion of free time and commitment to me and the development of this thesis. I am indebted to the technicians of the Solid State Electronics Lab--notably, Victor Swenson--for their assistance and support in the lab. Finally, I thank the Honors Program and staff for making this thesis possible.

Appendix: Further Processing Details

I. Photolithography

Adhesion promoter- 1:1 HMDS:AZ 1500 thinner.

Photoresist- AZ5214E.

Cycle: Pre-spin dehydration bake at 135°C 30 min. Ramp fast to 8000 rpm, hold for 5-10 seconds, reduce to 4000 rpm for remainder of 30 seconds. Apply AZ5214E and spin immediately at 4000 for 30 seconds.

Positive photolithography: post-spin bake on hot plate @80°C for 60 sec., expose on Karl Suss photolithography for 7.5s @28.3 mW/cm^2. Develop in 1:1 MF312:DI water.

Image reversal: post-spin bake on hot plate @90°C for 90 sec., expose on Karl Suss photolithography for 7.5 s @28.3 mW. Post-exposure bake on hot plate @115°C for 90 sec., flood expose (external filter in) on Karl Suss, develop in 1:1.2 MF312:DI water.

II. Electron-beam conditions:

pressure at 3 X 10^{-5} Torr, room temperature, 100 mA@10 kV.

III. Vacoflux sputtering conditions:

DC plasma sputtering system at a base pressure of 10^{-7} Torr in an Argon plasma at 200 cccm on a SiO_2 substrate at 200°C. The voltage across the plasma was regulated to give a constant current flow at 30 mA. At these conditions, the Fe-Co alloy was deposited at 125 Å/m for 8 minutes, yielding a film thickness of 1000 Å.

REFERENCES

1. A. Kantimahanti, Master of Science thesis, Weichold, 1992.
2. Friedlander, (personal communication), November 1992.
3. D.C. Jiles and D.L. Atherton, IEEE Trans. Magn. **MAG-19,** 2783-2185 (1983).
4. F. Ossart, T.A. Phung, and G. Meunier, J. Appl. Phys. **67**, (1990).
5. I.D. Mayergoyz and G. Friedman, IEEE Trans. Magn. **MAG-24**, 212 (1988).
6. M. Hodgdon, IEEE Trans. Magn. **MAG-24**, (1988).
7. K. Carpenter, IEEE Trans. Magn. **MAG-27**, (1991).
8. L. Solymar and D. Walsh, *Lectures on the Electrical Properties of Materials* (Oxford University Press, New York, 1988).
9. C. Paul and S. Nasar, *Introduction to Electromagnetic Fields* (McGraw-Hill Book Company, New York, 1987), p. 229.
10. D. O. Smith, J. Appl. Phys. **29**, (1958).
11. C. Kittel, Introduction to Solid State Physics (John Wiley and Sons, Inc., New York, 1986), p.397-460.
12. R. SooHoo, *Magnetic Thin Films* (Harper and Row Publishers, New York, 1965), p. 37-111
13. J.H. Van Vleck, Phys. Rev., **52**: 1178 (1937).
14. J.H.E. Grifiths, Oxford Conf. on Microwave Spectroscopy, July 1948; and, J.H.E. Griffiths, Physica, **17**: 253-258 (1951).
15. J.R. MacDonald, Phys. Rev., **81**: 312 (1951); and, J.R. MacDonald, Phys. Rev., **31**: 329 (1951).
16. T.G. Knorr and R.W. Hoffman, Phys. Rev., **113**: 1039 (1959).
17. C.D. Graham, Jr., in C.A. Neubauer et al. (eds.), *op. cit.*, p 288.
18. Segmüller, J. Appl. Phys., **32**: 89S(1961).

19. E. Banks, N.H. Riederman, H. W. Schleuning, and L.M. Silber, J. Appl. Phys. **32**, (1961).

20. F. B. Hagedorn, J. Appl. Phys. **30**, 2545 (1959).

21. F.B. Humphrey and E. M. Gyorgy, J. Appl. Phys. **30**, 935 (1959).

22. Vacoflux manual, (Vacuumschmelze, GMBH).

23. Wegerle, (personal communication), April 1993.